

Study of the impact of pre- and real-time deposition of lithium on plasma performance on NSTX

G.P. Canal^{1,2}, R. Maingi³, T.E. Evans¹, S.M. Kaye³, D.K. Mansfield³ and the NSTX team³

¹General Atomics, P.O. Box 85608, San Diego, CA 92186-5608, USA

²Oak Ridge Associated Universities, Oak Ridge, TN 37831, USA

³Princeton Plasma Physics Laboratory, Princeton, NJ, USA

Abstract—The efficiency of two lithium (Li) injection methods used on the National Spherical Torus Experiment are compared in terms of the amount of Li used to produce equivalent plasma performance improvements, namely Li evaporation over the divertor plates, prior to the initiation of the discharge, and real-time Li injection directly into the plasma scrape-off layer during the discharge. The measurements show that real-time injection is more efficient as it requires only a fraction of the amount of Li used by the evaporation method to improve plasma performance. The improvements of the real-time method, compared to the Li evaporation method, are: (i) significantly lower D_α light emission, which is an indication of lower particle recycling, (ii) about 20 % higher energy confinement, consistent with a reduction in the electron transport channel, and (iii) easier access to ELM suppression.

I. INTRODUCTION

Experiments in many machines have shown improvements on plasma confinement and edge stability when elemental lithium (Li) is used to coat the plasma facing components (PFCs) [1]–[20]. While some technologies have been developed to apply thin-film Li coatings onto PFCs prior to the initiation of the discharge [12], [13], other technologies have been designed to deposit Li into the plasma scrape-off layer (SOL) during the discharge, i.e. in real-time [1], [6]–[8].

On the National Spherical Torus Experiment (NSTX), three methods of introducing Li into the plasma were used in the past, namely pre-deposition via Li evaporation [12], [13], [15], real-time Li injection [16], and liquid Li divertor [18]. In this paper, the impact of pre- and real-time Li deposition on the performance of NSTX plasmas are compared in terms of the amount of Li used. In the first method, a Li thin-film is deposited over the lower divertor targets by evaporation, before the discharge, using a device named as “LITER” (LITHium Evaporator [12], [13]), which consists of a reservoir oven with an output duct inserted into a gap of the NSTX upper divertor, Fig 1(a-b). To provide liquid Li, the reservoir oven operated at temperatures between 550 °C and 650 °C, with the output duct operated about 50 °C to 100 °C hotter to reduce Li condensation. The evaporation rates obtained with this method are in the range of 1 to 40 mg/min, per LITER unit, with the rate being controlled by the reservoir oven temperature. The LITER central-axis aimed at the lower divertor and the Gaussian half-angle at $1/e$ of the measured evaporated Li angular distribution is about 11.5°, with the angular distribution of the evaporated

Li being independent of the Li reservoir oven temperature. In the second method, a Li aerosol is injected into the plasma scrape-off layer during the discharge using a device named as “Li Dropper” [16], which simply drops spherical Li powder into the plasma SOL by gravitational acceleration in a controllable manner using a vibrating piezoelectric disk with a central aperture, Fig 1(c). In these studies, a powder of spherical Li particles of 44 μm of average diameter were used. To avoid uncontrolled reaction with air, the Li particles were coated with a 30 nm mantle of microcrystalline Li_2CO_3 , such that the particles are 99.9% Li and 0.1% Li_2CO_3 in composition. The injection rates obtained with this method are in the range 1 to 120 mg/s, per Dropper unit, with the rate depending on the voltage applied to the opposite sides of the vibrating piezoelectric disk. The Dropper has been used to inject Li in three machines: NSTX [16], EAST [19] and DIII-D [20]. Fig 1(d-f) shows visible light images, from a toroidal view, of plasma cross-sections in these three machines. The dominant green emission in the images come from singly ionized Li (Li II, 548.5 nm), which is relatively evenly distributed around the plasma despite the localization of the Li particle source that, in these discharges, is located at the top of the machine. Emission from neutral Li is also visible in the inner divertor region (Li I, 670.8 nm). Compared to the Li thin-film pre-deposition method, the real-time injection of Li aerosol has the advantage of replacing, in real-time, the Li thin-film removed from the PFCs by the plasma. In the NSTX discharges described in this paper, the LITER evaporated Li for several minutes prior to the initiation of the discharges, while the Li Dropper operated for only about 1 second, which is the typical duration of an NSTX discharge. Therefore, the total amount of Li used by these two methods are comparable.

II. DESCRIPTION OF THE EXPERIMENTS

To compare the impact of pre-deposition and real-time Li injection on plasma performance, three NSTX H-mode discharges with similar global plasma parameters were selected: (i) the reference discharge, which had no Li injected, #132549; (ii) a discharge that used the LITER to evaporate 100 mg of Li prior to the initiation of the discharge, #135047; and (iii) a discharge that used the Li Dropper with 110 mg/s of injection rate, #135058. For the LITER discharge, two LITER units, installed 150° apart, were used on NSTX

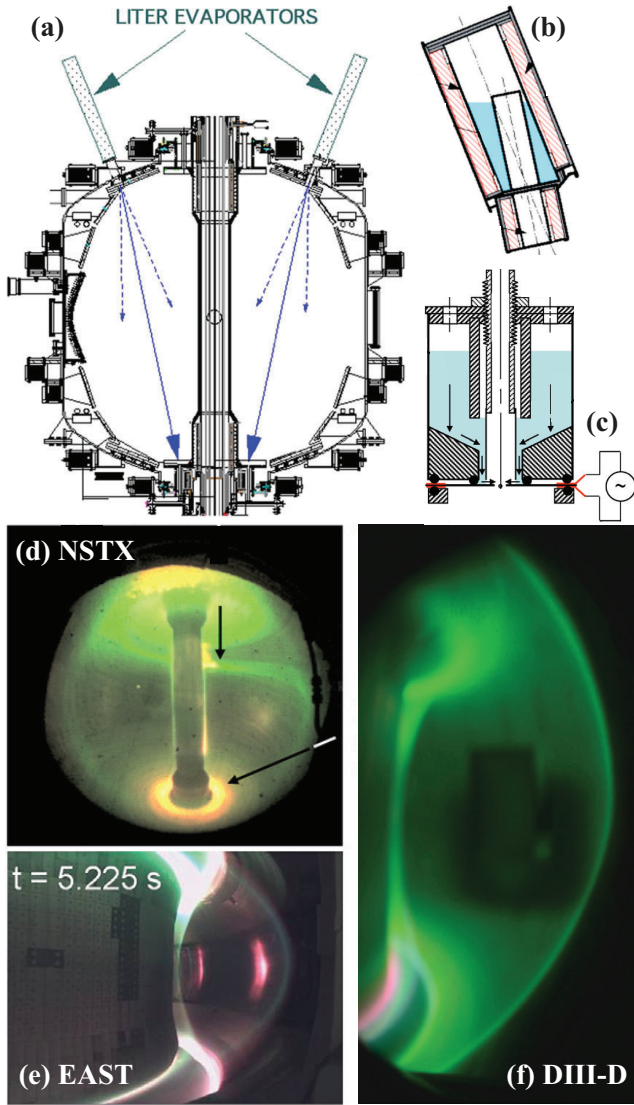


Fig. 1. (a) NSTX cross-section showing two LITER units. Schematic drawings of (b) the LITER and (c) Dropper. Visible light image, from a toroidal view, of plasma cross-sections in (d) NSTX, (e) EAST and (f) DIII-D plasmas, with the Dropper in operation. Images shown in (a-f) are reproduced from [12], [13], [16], [19] and [20].

to increase the evaporation rate, Fig 1(a). Additionally, the reference and LITER discharges had 5 minutes of He glow wall conditioning. In these three NSTX discharges, the ion ∇B drift direction pointed towards the x-point and the global plasma parameters were: minor radius $a = 0.60$ m, elongation $\kappa = 2.3$, top triangularity $\delta_{\text{top}} = 0.42$, bottom triangularity $\delta_{\text{bot}} = 0.75$, safety factor at 95% of the normalized poloidal flux $q_{95} = 8.5$, toroidal magnetic field at the vacuum vessel geometrical center $B_0 = 0.44$ T, plasma current $I_P = 1.0$ MA, Fig. 2(a), and neutral beam injected power $P_{\text{NBI}} = 4.0$ MW, Fig. 2(b).

III. RESULTS

The first indication of changes on particle recycling and plasma edge stability due to the Li injection method can be seen in the D_α light emission, Fig. 2(c). The measurements

show a significant reduction in the D_α emission when Li is injected using the Dropper, while a modest decrease is observed when the LITER was used. The Dropper also seems to facilitate the suppression of edge localized modes (ELMs). Although ELM suppression was achieved in several NSTX discharges using the LITER [12], [13], [15], 100 mg of evaporated Li was usually insufficient to suppress ELMs in NSTX [21]. Note that the reduction in the D_α light emission caused by the Dropper occurs very early in the discharge such that the amount of Li injected is only about 30% of that used by the LITER.

Another important effect associated with the injection of Li is the control of core fueling. Thomson scattering measurements of the electron density at the plasma center, n_{e0} , show a significant reduction in its rate of change, dn_{e0}/dt , when Li is injected, Fig. 2(d), but no significant differences are found between LITER and Dropper. The results also show an increase of about 20% in the plasma stored energy, W_{MHD} , normalized plasma pressure, β , energy confinement time, τ_E , and energy confinement enhancement factor, $H_{98y,2}$, when the Dropper is used, Fig. 2(e-h). Although the measurements show just a modest improve in energy confinement when the Dropper is used, note that this improvement is obtained with just a fraction of the amount of Li used by the LITER. The maximum value of the normalized β , β_N , during both the LITER and Dropper discharges, is about 25% higher than in the reference discharge. However, albeit β is larger in the Dropper discharge, β_N is not significantly different during both the LITER and Dropper discharges, Fig. 2(i). This occurs because the plasma minor radius in the Dropper discharge decreased slightly, with respect to the LITER discharge, causing the value of β_N in both discharges to be comparable. Here, $\beta_N = \beta [\%] a [\text{m}] B_0 [\text{T}] / I_P [\text{MA}]$ and the normalized plasma pressure $\beta = 2\mu_0 \langle p \rangle / \bar{B}^2$, with $\langle p \rangle = \frac{1}{V} \int p dV$ being the volume averaged plasma pressure, \bar{B} the mean magnetic field at the plasma boundary and μ_0 the vacuum magnetic permeability. The observed improvement in energy confinement is reflected in the maximum values of the central electron, T_{e0} , and ion, T_{i0} , temperatures achieved during the discharge, Fig. 2(j-k). The results also show that the plasma rotates faster in the center when Li is injected, but the evolution of the central plasma rotation, $V_{\phi 0}$, in the Dropper discharge is not significantly different from that in the LITER discharge, Fig. 2(l).

In order to compare the plasma kinetic radial profiles from these NSTX discharges, and due to the observed difference in the evolution of n_{e0} , the profiles were taken from slightly different times in the discharges, namely 0.47-0.52 s for the reference discharge, 0.64-0.67 s for the LITER discharge, and 0.53-0.58 for the Dropper discharge. With these selected time windows, the electron number density, n_e , profiles from the three discharges overlay reasonably well, Fig. 3(a). The measurements show that the plasma rotation, V_ϕ , increases across the plasma radius when Li is injected but no significant difference is observed between the two Li injection methods, Fig. 3(b). The fact that the

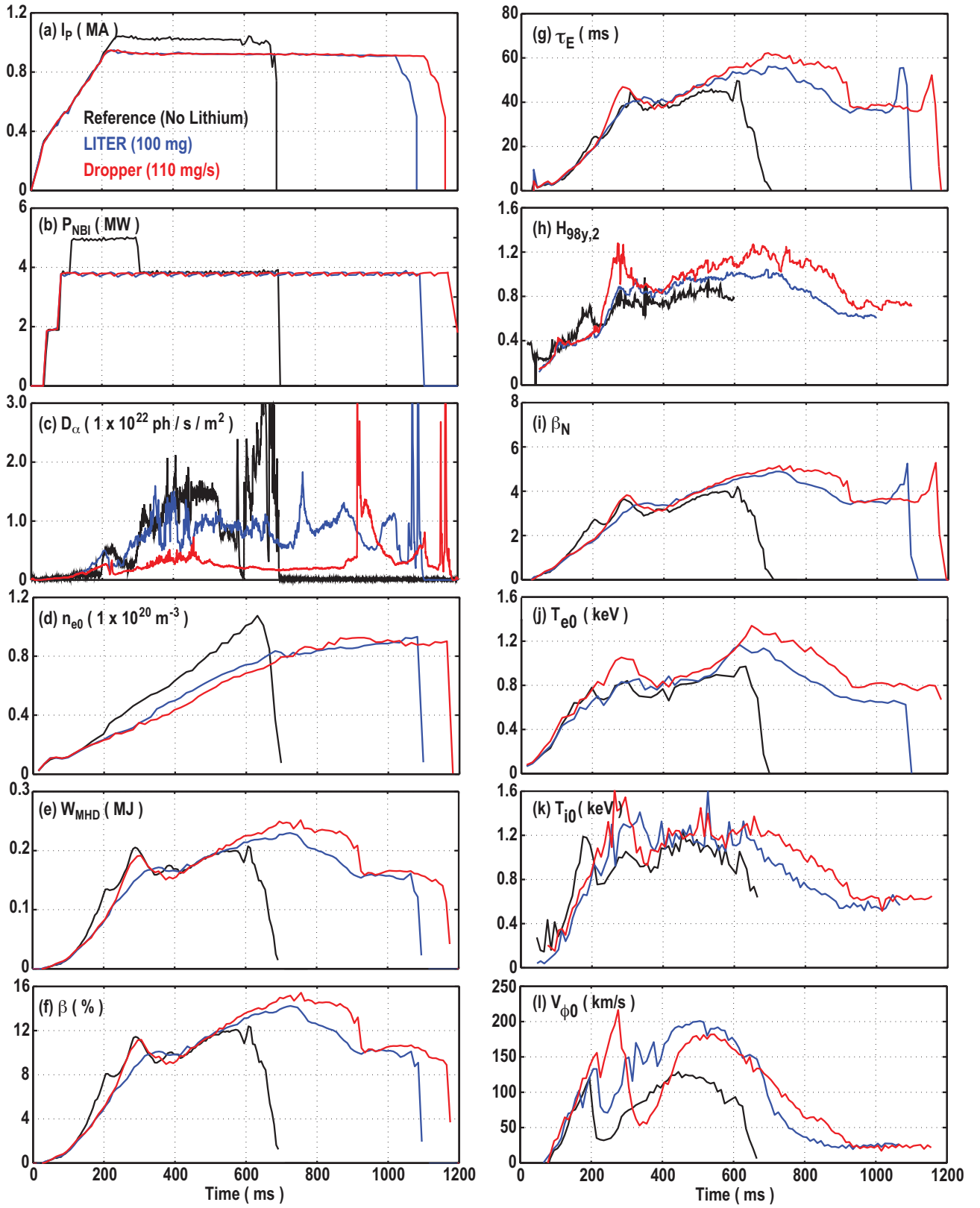


Fig. 2. Time traces of (a) plasma current, (b) neutral beam injected power, (c) D_α light emission intensity, (d) central electron density, (e) plasma stored energy, (f) normalized plasma pressure, (g) energy confinement time, (h) energy confinement enhancement factor, (i) normalized β , central (j) electron and (k) ion temperatures, and (l) central plasma rotation, for three NSTX discharges: #132549 (No Lithium), #135047 (LITER with 100 mg) and #135058 (Dropper with 110 mg/s).

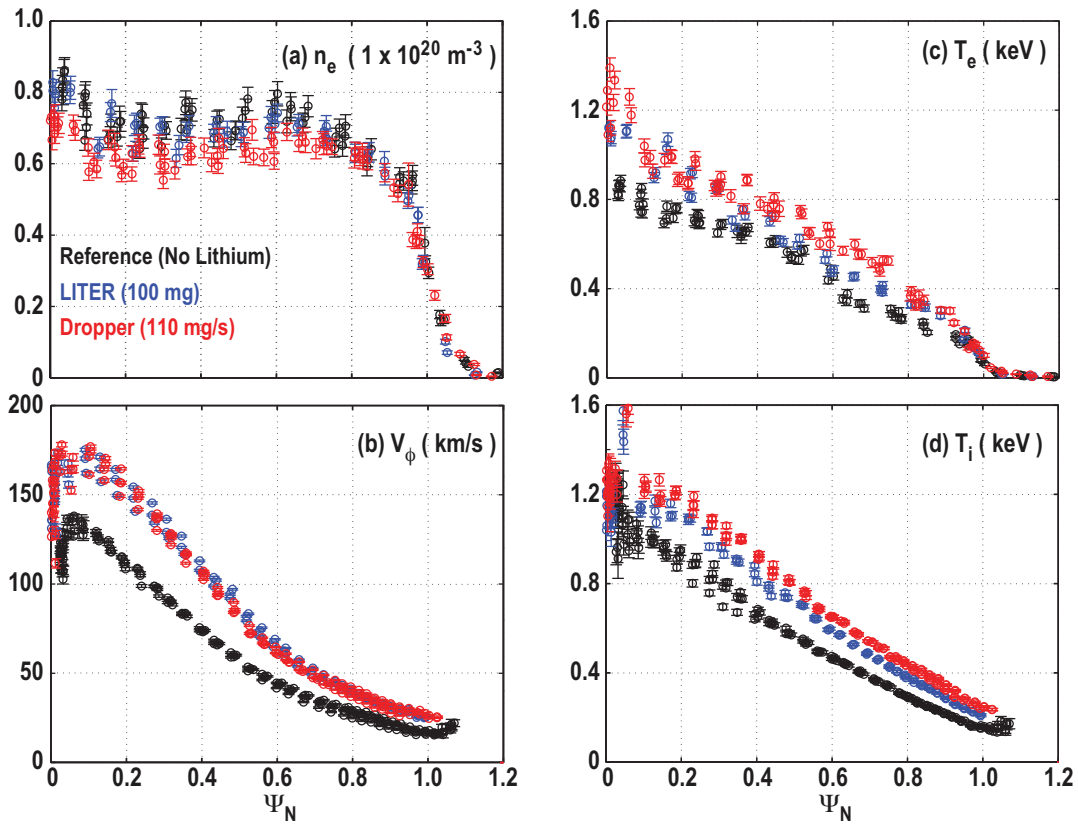


Fig. 3. Radial profiles of (a) electron number density, (b) plasma rotation, and (c) electron and (d) ion temperatures for three NSTX discharges: #132549 (No Lithium), #135047 (LITER with 100 mg) and #135058 (Dropper with 110 mg/s).

plasma rotates faster when Li is injected might result from a reduced drag caused by the lower number of charge exchange processes due to the lower recycling. However, to explain the very similar effect of both Li injection methods on the V_ϕ profile, the amount of Li injected in these discharges must be large enough to cause the contribution of charge exchange processes to the torque balance to be negligible, causing V_ϕ to be independent of the Li injection method. The electron, T_e , and ion T_i , temperature profiles are higher than in the reference discharge, with T_e and T_i in the Dropper discharge being modestly higher than in the LITER discharge across most of the plasma core, Fig. 3(c-d). The increase in T_e and T_i in the Dropper discharge reflects the improvement in energy confinement discussed previously, and shown in Fig. 2(e-h).

To better understand the effect of the Li injection method on the plasma confinement, diffusive cross-field transport coefficients were estimated for these three NSTX discharges using the plasma transport code TRANSP [23]. The calculations show, for both Li injection methods, a strong reduction in the electron thermal diffusivity, χ_e , in the plasma core ($\Psi_N \leq 0.5$), Fig 4(a). The ion thermal diffusivity, χ_i , however, is found to increase when Li is injected, Fig 4(b). The calculations show that, when the Dropper is used, a reduction in χ_e , with respect to the LITER discharge, is obtained for $\Psi_N \geq 0.6$, while an increase in χ_i is found in the same location. To explain the observed improvement

in the energy confinement when Li is injected into the plasma, the reduction in the electron heat transport channel must compensate the increase in the ion heat transport channel. Note that, in the plasma edge, the two-fluid thermal diffusivities χ_e and χ_i can sometimes be dominated by the electron-ion energy exchange (equipartition) term, which usually has larger uncertainties in the edge region. To avoid this issue, one can calculate the effective thermal diffusivity, χ_{eff} , which combines the two species into a single-fluid, thereby canceling the energy exchange term. The χ_{eff} is, therefore, a more reliable indicator of the overall change in the plasma energy transport. As shown in Fig 4(c), the calculations show a significant reduction in χ_{eff} in the plasma core ($\Psi_N \leq 0.5$), thus confirming the results from the two-fluid calculations. For $\Psi_N \geq 0.7$, the calculations show an increase in energy transport in the LITER discharge, with respect to the reference, while the Dropper reduces the energy transport by half of that in the reference. The momentum confinement is also affected by the injection of Li. The toroidal momentum diffusivity, χ_ϕ , decreases by almost half of that in the reference for $\Psi_N \geq 0.6$ when Li is injected, Fig 4(d). However, no significant differences between LITER and Dropper are observed.

The impact of the Li injection method on the impurity accumulation and radiated power was also addressed in this work. The measurements show that the radiated power, P_{rad} , in the reference discharge is significantly higher than in

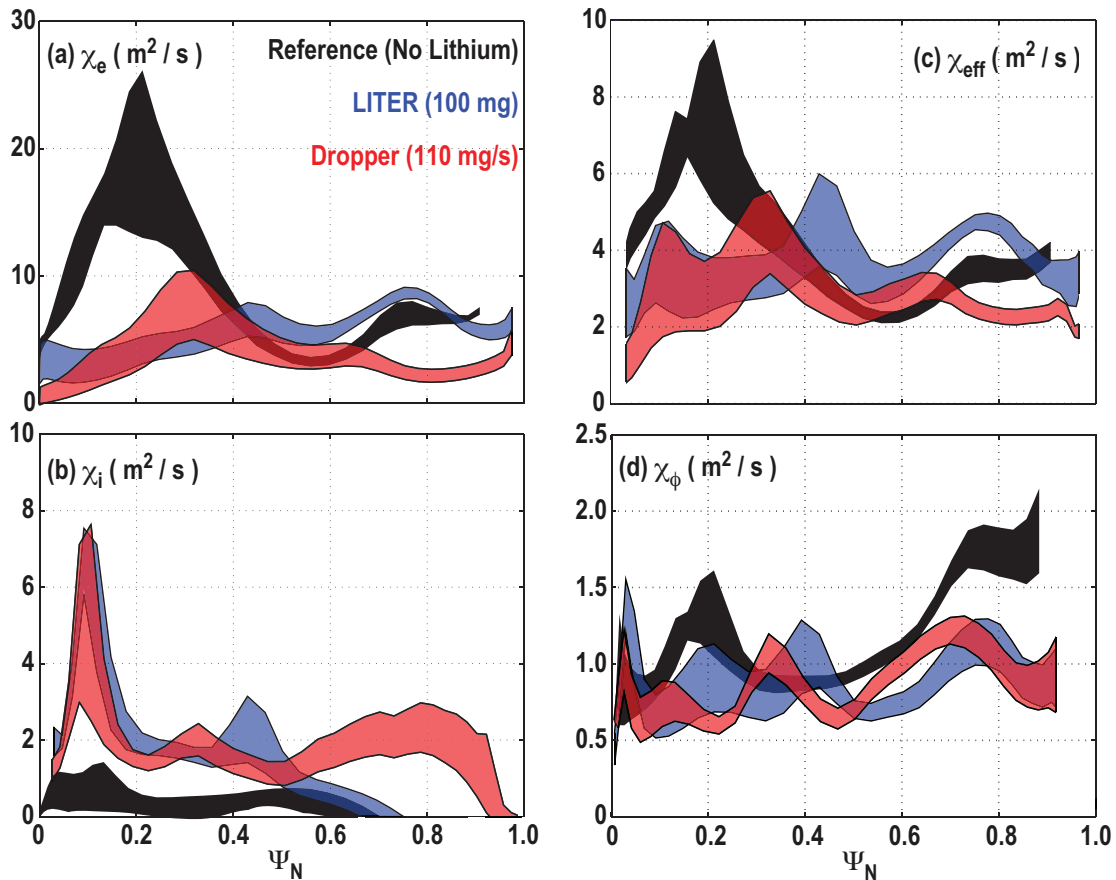


Fig. 4. Radial profiles of (a) electron and (b) ion thermal diffusivities, (c) effective (single-fluid) thermal diffusivity, and (d) momentum diffusivity for three NSTX discharges: #132549 (No Lithium), #135047 (LITER with 100 mg) and #135058 (Dropper with 110 mg/s). For completeness, the TRANSP runs are: A10 for the reference discharge (#132549), A07 for the LITER discharge (#135047) and A04 for the Dropper discharge (#135058).

the LITER and Dropper discharges, Fig. 5(a). This is a consequence of the higher values of n_e and lower values of T_e and T_i in the reference discharge. Although P_{rad} in both LITER and Dropper discharges is lower than in the reference discharge, no significant difference is found in P_{rad} between these two Li injection methods. The high-Z impurity density, n_Z , is found to be higher in the reference discharge than in the LITER and Dropper discharges, Fig. 5(b). However, since n_e in the reference discharge is also higher than in the LITER and Dropper discharges, the high-Z impurity concentrations at the plasma center, n_Z/n_e , of the three discharges are comparable, Fig. 5(c). After about 600 ms, the value of n_Z for the Dropper discharge is found to be slightly larger than in the LITER discharge, which is thought to be caused by the ELM suppression induced by the Dropper.

Measurements of the carbon density, n_C , profiles in the three discharges are very similar for most of the plasma core, Fig. 5(d). The measurements show only a small difference in the plasma edge, where the Dropper discharge has a slight higher value of n_C than the LITER discharge. Again, this might also result from the ELM suppression achieved with the Dropper. The same behavior is observed in the effective ion charge, Z_{eff} , which is higher in the Dropper discharge

than in the LITER discharge not only in the plasma edge but across the plasma radius, Fig. 5(e). This results from the slightly lower values of n_e for the selected time in the Dropper discharge, Fig. 3(a).

IV. SUMMARY

Improvements in plasma confinement and edge stability have been observed in several machines when elemental Li is used to coat the PFCs. On NSTX, such improvements were observed when Li was evaporated into the machine, and pre-deposited on the divertor targets prior to the initiation of the discharge, and also during real-time injection, where Li was injected directly into the plasma SOL. In this paper, the efficiency of these two Li injection methods are compared in terms of the amount of Li used to produce equivalent plasma performance improvements.

The measurements show that both Li injection methods lead to comparable reductions in dn_{e0}/dt , which is an indication of particle fueling, they both increase plasma rotation by about the same factor and they both lead to similar reductions in radiated power and impurity accumulation. The measurements, however, show that the Dropper causes a significantly larger reduction in the D_α light emission, and consequently in particle recycling, than the LITER. In

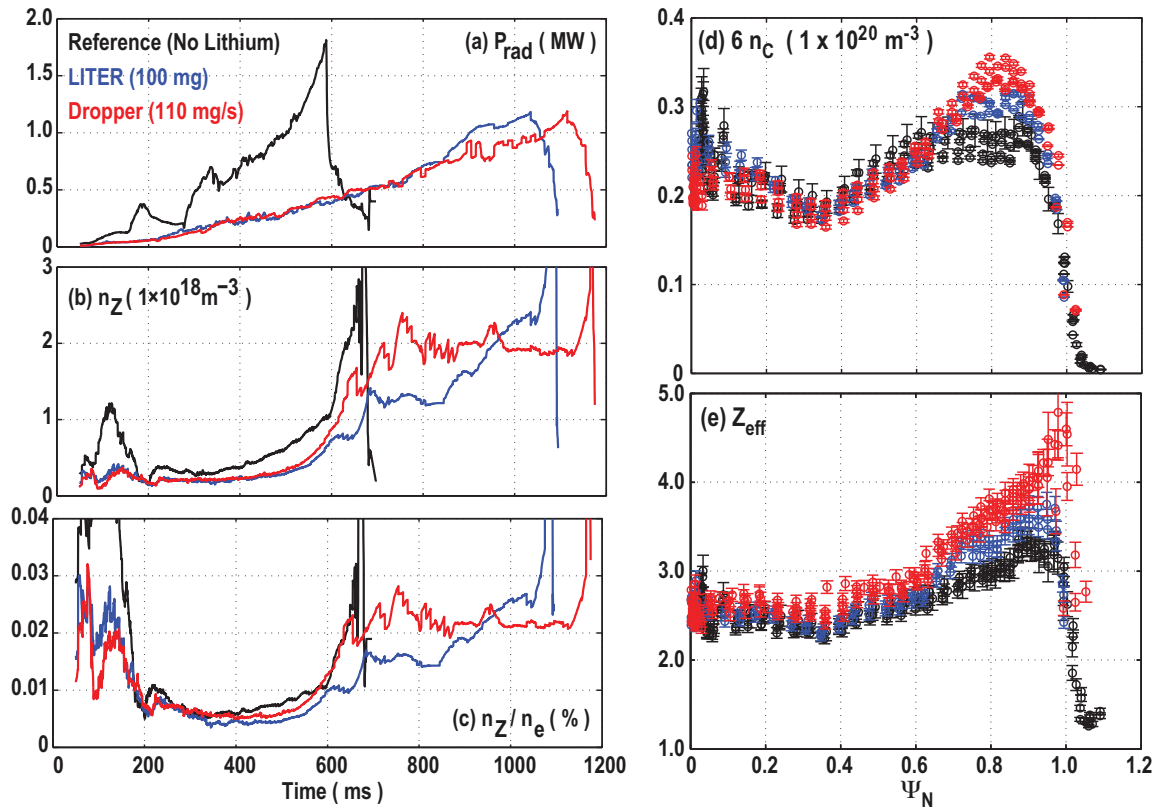


Fig. 5. Time traces of (a) radiated power and high-Z impurity (b) density and (c) concentration in the plasma core for three NSTX discharges: #132549 (No Lithium), #135047 (LITER with 100 mg) and #135058 (Dropper with 110 mg/s). Radial profiles of (d) carbon density and (e) effective ion charge for the same three NSTX discharges.

addition, ELM suppression was achieved with the Dropper. Although ELM suppression was achieved in several NSTX discharges using the LITER, 100 mg of evaporated Li was insufficient to suppress ELMs in this specific discharge. The results also show that the Dropper leads to about 20 % higher energy confinement than the LITER. This increase is correlated with a decrease in the electron transport channel. All these observations show that the Dropper can affect recycling, confinement and edge stability of NSTX plasmas in a more efficient way than the LITER, as it requires only a fraction of the amount of Li used by the LITER. When the Dropper is used, the Li that is directly injected into the plasma SOL during the discharge is transported by the plasma to the targets. This method has, therefore, the advantage of replacing, in real-time, the Li thin-film removed from the PFCs by the plasma, which is thought to be the cause of the observed higher efficiency of the Dropper to produce equivalent improvements in plasma performance to those obtained with the LITER.

ACKNOWLEDGMENTS

This research was supported by the General Atomics Postdoctoral Research Participation Program administered by ORAU and is part of the General Atomics Collaboration on Plasma Boundary Interfaces and Macroscopic Stability at NSTX-U. This work has been supported by the US Department of Energy, Office of Science, Office of Fusion

Energy Science under DOE award DE-SC0012706 and DOE contract DE-AC02-09CH11466.

REFERENCES

- [1] B. Terreault *et al.*, *Journal of Nuclear Materials* **220** (1995) 1130
- [2] D.K. Mansfield *et al.*, *Physics of Plasmas* **2** (1995) 4252
- [3] H. Sugai *et al.*, *Journal of Nuclear Materials* **220** (1995) 254
- [4] D. Mansfield *et al.*, *Nuclear Fusion* **41** (2001) 1823
- [5] S. I. Krasheninnikov *et al.*, *Physics of Plasmas* **10** (2003) 1678
- [6] V.A. Evtikhin *et al.*, *Plasma Physics and Controlled Fusion* **44** (2002) 955
- [7] S.V. Mirnov *et al.*, *Fusion Engineering and Design* **65** (2003) 455
- [8] S.V. Mirnov *et al.*, *Plasma Physics and Controlled Fusion* **48** (2006) 182
- [9] R. Majeski *et al.*, *Physical Review Letters* **97** (2006) 075002
- [10] F.L. Tabarés *et al.*, *Plasma Physics and Controlled Fusion* **50** (2008) 124051
- [11] G. Mazzitelli, 22nd IAEA Fusion Energy Conference, 2008 (Geneva, Switzerland, 13-18 October), CD-ROM file EX-P4-6 (http://www-pub.iaea.org/MTCD/Meetings/FEC2008/ex_p4-6.pdf)
- [12] H.W. Kugel *et al.*, *Physics of Plasmas* **15** (2008) 056118
- [13] H.W. Kugel *et al.*, *Journal of Nuclear Materials* **390** (2009) 1000
- [14] Y. Hirooka *et al.*, *Journal of Nuclear Materials* **390** (2009) 502
- [15] R. Maingi *et al.*, *Physical Review Letters* **103** (2009) 075001
- [16] D.K. Mansfield, *Fusion Engineering and Design* **85** (2010) 890
- [17] R. Maingi *et al.*, *Nuclear Fusion* **52** (2012) 083001
- [18] M. Jaworski *et al.*, *Nuclear Fusion* **53** (2013) 083032
- [19] J.S. Hu *et al.*, *Physical Review Letters* **114** (2015) 055001
- [20] T.H. Osborne *et al.*, *Nuclear Fusion* **55** (2015) 063018
- [21] R. Maingi *et al.*, *Journal of Nuclear Materials* **463** (2015) 1134
- [22] R. Maingi *et al.*, *Fusion Engineering and Design* **117** (2017) 150
- [23] R.J. Hawryluk, *Physics of Plasmas Close to Thermonuclear Conditions* **1** (1980) 19